PCCP

Accepted Manuscript

ROYAL SOCIETY OF CHEMISTRY

www.rsc.org/pccp

Graphical Abstract

Water-soluble 1,2,4-Triazole with Diethylene Glycol Monoethyl Ether Groups: Synthesis, Characterization and Application as Electron Injection Layer for PLEDs

Chia-Shing Wu, Yu-Sing Wu and Yun Chen*

Department of Chemical Engineering, National Cheng Kung University, Tainan, Taiwan

*Corresponding author: yunchen@mail.ncku.edu.tw

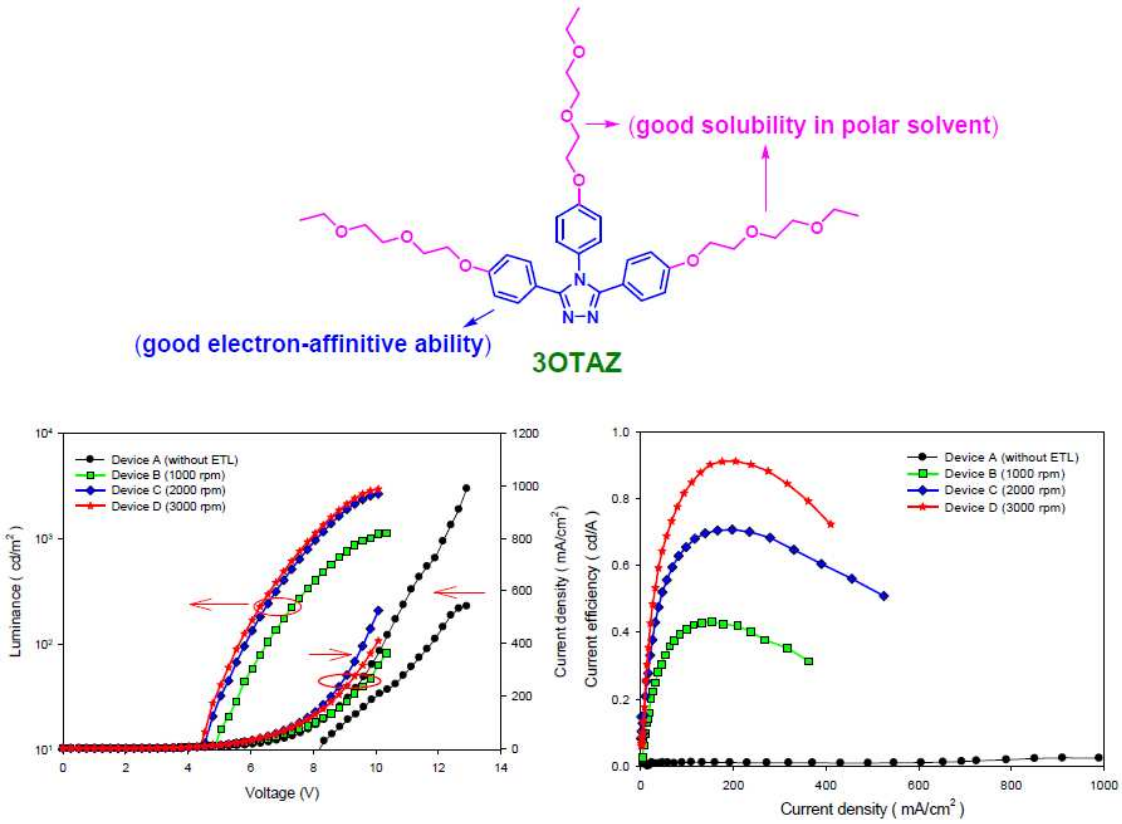

Novel electron injection material **3OTAZ** composed of aromatic 1,2,4-triazolyl core with three diethylene glycol ether groups enhances electroluminescence of HY-PPV.

Water-soluble 1,2,4-Triazole with Diethylene Glycol Monoethyl Ether Groups: Synthesis, Characterization and Application as Electron Injection Layer for PLEDs

Chia-Shing Wu, Yu-Sing Wu and Yun Chen*

Department of Chemical Engineering, National Cheng Kung University, Tainan, Taiwan

*Corresponding author: yunchen@mail.ncku.edu.tw

Abstract

We design a novel electron injection material **3OTAZ** composed of aromatic 1,2,4-triazolyl core with three diethylene glycol ether groups to enhance electroluminescence of PLEDs using environmentally stable aluminum cathode. Multilayer PLEDs [ITO/PEDOT:PSS/HY-PPV/EIL(**3OTAZ**)/Al] using **3OTAZ** as electron injection layer (EIL) exhibit significantly enhanced device performance. The maximum luminous power efficiency and maximum luminance of the device with **3OTAZ** as EIL were enhanced to 0.34 lm/W and 2970 cd/m^2, respectively, compared with those without EIL (0.006 lm/W, 230 cd/m^2). The turn-on voltage was also significantly reduced from 8.2 V to 4.3 V simultaneously. The performance enhancement has been attributed to improved electron injection which has been confirmed by the raise in open-circuit voltage (V_{oc}) obtained from photovoltaic measurements. Moreover, more balanced charges injection and transport has been achieved by inserting **3OTAZ** which adjust hole-blocking effect investigated by hole-only devices. The results indicate that **3OTAZ** is an excellent electron injection candidate in performance enhancement for PLEDs with high work function Al cathode.

Introduction

For more than two decades, polymer light-emitting diodes (PLEDs)[1-3] have attracted continuous attention because of their low cost, easy processability, and the possibility of easily fabricating flexible, large-area displays. PLEDs are carrier injection devices, which basically require balanced hole and electron injection from the anode and the cathode respectively, and their fast transport and recombination in the emissive layer.[4,5] To achieve high device efficiency, it is necessary that both electrons and holes are efficiently injected.[5,6] Therefore, substantial improvements in the device efficiency have been obtained upon modification of the anode,[7-9] by the introduction of low-work function cathodes,[10] and by using hole and electron injecting/transporting layers.[11–14] Efficient injection of electrons from the cathode to emissive conjugated polymers plays an important role in improving the device efficiency and stability. For most conjugated polymers, hole injection is more favorable than electron injection.[11,15] Therefore, low work-function metals such as Ba and Ca are the widely utilized cathode materials to facilitate efficient electron injection. However, those metals are very sensitive to moisture and oxygen and probably form detrimental quenching sites near the interface between the emission layer (EML) and the cathode.

To overcome these problems, the cathode should be stable to environment, the environmentally stable high-work-function metals such as Al, Cu, Ag, and Au as the cathode has attracted extensive attention recently. However, electron injection from cathode is usually hindered by its high work-function. Therefore, use of a water- or alcohol-soluble electron injection layer (EIL) based on a conjugated polymer grafted with amino, ammonium salt, or diethanolamino groups has been demonstrated to allow the use of a high-work-function metal as the cathode.[16-23] This is because interfacial dipole or space charge is formed between the emitting layer (EML) and the cathode that reduces the electron injection barrier. In addition, crown ether groups may be expected to serve the same purpose.

Crown ethers are a special class of ether able to form stable complexes with alkali, alkaline-earth, and transition-metal ions.[24,25] Chen et al. first reported the use of water/methanol-soluble polyfluorene grafted with 18-crown-6 as the electron-injection layer (EIL) for deep-blue-emission PLEDs, allowing the use of environmentally stable Al as the cathode.[26]

Moreover, ethylene glycol groups also shows good solubility in highly polar solvents and poly(ethylene glycol)-based surfactants demonstrate performance enhancement for PLEDs using high-work-function metal aluminum as cathode.[27] Among the typical electron-affinitive materials, aromatic 1,2,4-triazolyl based derivatives show good thermal and chemical stabilities, leading to their common use as electron injection/transport and hole-blocking materials in LEDs.[28-30] However, their solubility in solvents are quite limited, especially in mixture of water and alcohol. Solubility in water or alcohol is a requirement for electron-injection material to be spin-coated on top of emission layer. Otherwise, subsequent solvents will damage the emission layer by partial dissolution. By introducing ethylene glycol ether groups to aromatic 1,2,4-triazolyl core, its solubility in alcohol can be further enhanced.

Recently, most of the water- or alcohol-soluble electron injection materials mainly based on polymers are developed and demonstrated.[16-23,26,27] Nonetheless, a few researches focus on small molecule have been reported.[30l] In particular, small-molecular-weight materials have received interest due to their easy purification by re-crystallization or column chromatographic techniques, and mono-disperse with well-defined chemical structures, and synthetically well-reproducibility. In this study, we propose the use of a alcohol-soluble and small-molecule 1,2,4-triazole-based **3OTAZ** with diethylene glycol monoethyl ether groups as the EIL in PLEDs with HY-PPV (PDY-132, Merck[31,32]) as emitting layer (EML). The solubility in highly polar solvents (e.g., alcohol) provided by diethylene glycol monoethyl ether can prevent dissolution of the EML having a thin EIL atop it, and the

1,2,4-triazole parts with electron-affinitive ability to reduce the electron-injection barrier from a stable metal cathode (e.g., Al, Ag or Au) and to facilitate electron injection. When the **3OTAZ** was inserted between the emitting layer and the Al cathode as an EIL, the device efficiency was efficiently enhanced. The maximum luminance, maximum current efficiency and maximum luminous power efficiency were 2970 cd/m^2, 0.91 cd/A, and 0.34 lm/W, respectively, which were greatly superior to those without electron injection layer (230 cd/m^2, 0.02 cd/A, 0.006 lm/W). The results indicate that the **3OTAZ** is a promising electron injection layer for high performance PLEDs with high work function Al cathode.

Experimental Section

Materials

N,N-Dimethylformamide (DMF), methyl alcohol , di(ethylene glycol)monoethyl ether, chloroform, isopropyl alcohol, dimethyl sulfoxide, acetone, and acetonitrile were purchased from Tedia Chemicals and used as received. Hydrazine hydrate (Lancaster), 4-fluoroaniline (Alfa Aesar), 4-fluorobenzoic chloride (Acros), N-methyl-2-pyrrolidone (Janssen), phosphorus pentachloride (RDH), NaH (Acros), ethyl alcohol (Echo), N,N'-dimethylaniline (Acros), toluene (Echo), potassium bromide (Showa), ferrocene (Acros), tetra-*n*-butylammonium perchlorate (TCI), acetone (J. T. Backer) were from commercial sources and used without further purification. Hole-injection material poly(3,4)-ethylendioxythiophene-polystyrenesulfonate (PEDOT:PSS) and yellow-emitting material Livilux PDY-132 (Super Yellow; HY-PPV) were acquired from Bayer and Merck, respectively.

Measurements

All new synthesized compounds were identified by ^{1}H NMR, ^{13}C-NMR, FT-IR spectra, elemental analysis (EA) and Mass spectroscopy (MS). The ^{1}H and ^{13}C NMR spectra were obtained on a Bruker AMX-400 MHz spectrometer, with the chemical shifts reported in

ppm using tetramethylsilane (TMS) as an internal standard. The FT-IR spectra were measured as KBr disk on a Fourier transform infrared spectrometer, model 7850 from Jasco. The elemental analysis was carried out on a Heraus CHN-Rapid elemental analyzer. Thermogravimetric analysis (TGA) of samples was performed under nitrogen atmosphere at a heating rate of 10 °C/min using a PerkinElmer TGA-7 thermal analyzer. Thermal transition properties of samples were investigated using a differential scanning calorimeter (DSC), Mettler Toledo DSC 1 Star^{e} System, under nitrogen atmosphere at a heating rate of 10 °C/min. Absorption and photoluminescence (PL) spectra were measured with a Jasco V-550 spectrophotometer and a Hitachi F-4500 fluorescence spectrophotometer, respectively. Cyclic voltammograms were recorded with a voltammetric analyzer (model CV-50W from Bioanalytical Systems, Inc.) at room temperature under nitrogen atmosphere. The measuring cell was made up of a polymer-coated ITO glass as the working electrode, an Ag/AgCl electrode as the reference electrode, and a platinum wire as the auxiliary electrode. The electrodes were immersed in acetonitrile containing 0.1 M (n-Bu)$_4$NClO$_4$ as electrolyte. The energy levels were calculated using the ferrocene (FOC) value of -4.8 eV with respect to vacuum level, which is defined as zero. An atomic force microscope (AFM), equipped with a Veeco/Digital Instrument Scanning Probe Microscope (tapping mode) and a Nanoscope Ⅲa controller, was used to examine the morphology and to estimate the thickness and root-mean-square (rms) roughness of deposited films. The film thicknesses of electron injection and emitting layers were measured by a surface profiler (α-step 500).

Synthesis of Electron-Injection Material 3OTAZ (Scheme 1)

A mixture of 3,4,5-tris(4-fluorophenyl)-4H-1,2,4-triazole **(3**: 1.45 g, 4.11 mmol), di(ethylene glycol) monoehtyl ether **(**2.42g, 18 mmol), and NaH 50% (0.86 g, 18 mmol) with DMF (10 mL) as solvent was stirred at 130 °C for 24 h under a nitrogen atmosphere**.** The mixture was poured into a large amount of distilled water. The appearing precipitates were collected by filtration and then recrystallized from DMSO and water to afford

compound **3OTAZ** (Yield: 80.1%). ^{1}H-NMR (DMSO-d_6, ppm): δ 7.31~7.28 (m, 6H, Ar-H), 7.00 (d, 2H, *J* = 9.0 Hz, Ar-H), 6.91 (d, 4H, *J* = 9.0 Hz, Ar-H), 4.10~4.06 (m, 6H, -CH$_2$-), 3.74~3.69 (m, 6H, -CH$_2$-), 3.58~3.54 (m, 6H, -CH$_2$-), 3.49~3.46 (m, 6H, -CH$_2$-), 3.44~3.39 (m, 6H, -CH$_2$-), 1.07 (t, 9H, -CH$_3$). ^{13}C-NMR (DMSO-d_6, ppm): δ 159.43, 159.01, 154.13, 129.89, 129.70, 127.81, 119.72, 115.47, 114.55, 70.13, 70.08, 69.33, 68.96, 67.37, 65.68, 40.20, 40.03, 39.86, 39.70, 39.53, 39.36, 39.20, 15.22. Anal. Calcd. for $C_{38}H_{51}N_3O_9$: C, 65.78%; H, 7.41%; N, 6.06%. Found: C, 66.11%; H, 7.72%; N, 5.86%.

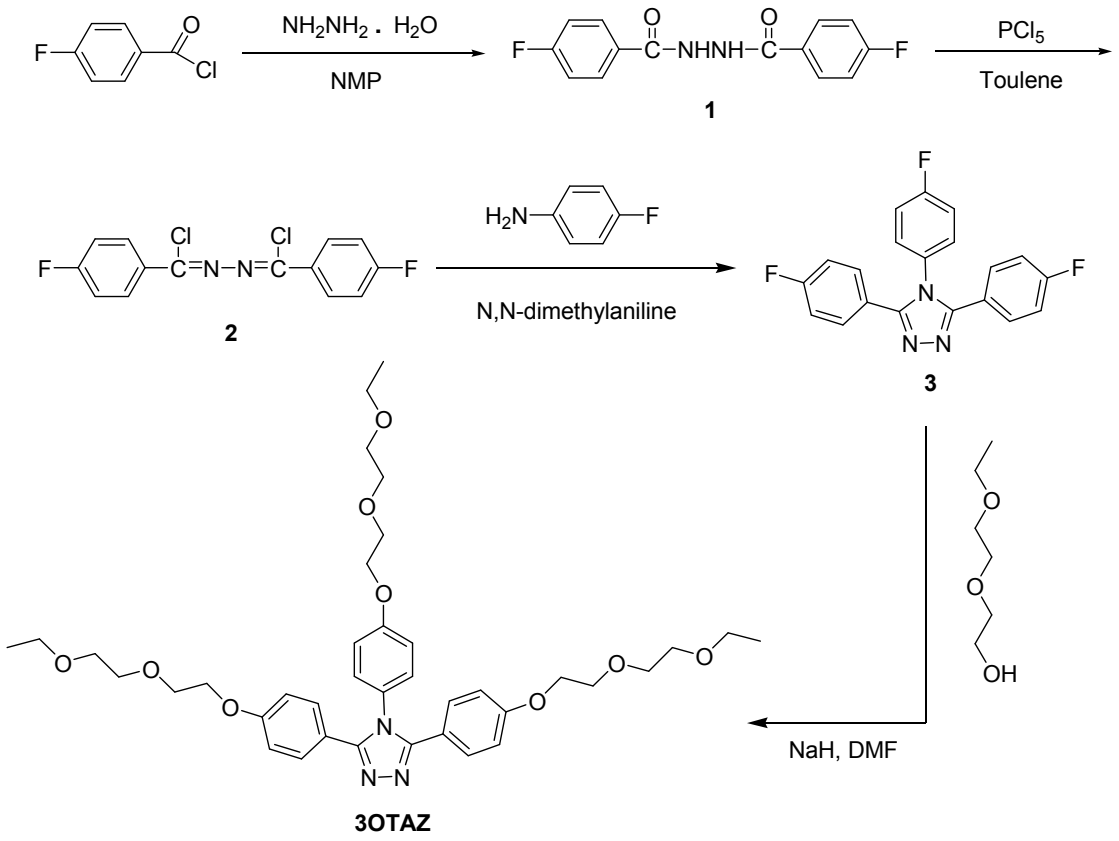

Scheme 1. Synthetic procedures of **3OTAZ**.

Fabrication of Polymer Light-Emitting Diodes

Multilayer polymer light-emitting diodes (PLEDs), with a structure of ITO/PEDOT:PSS/HY-PPV/**3OTAZ**/Al, were fabricated by the wet processes for the

investigation of optoelectronic characteristics. The glass substrate coated with an ITO conductive layer was used as the anode, the poly(3,4-ethylenedioxythiophene):polystyrenesulfonate (PEDOT:PSS, Bayer) as the hole-injection layer, the Livilux PDY-132 (HY-PPV, Merck) as the light-emitting layer, the **3OTAZ** as the electron-injection layer, and aluminum as the metal cathode. The ITO-coated glasses were washed successively in an ultrasonic bath of neutral cleaner/de-ionized water mixture, de-ionized water, acetone and 2-propanol, followed by treatment in a UV-ozone chamber. A thick hole-injection layer of PEDOT:PSS was spin-coated on top of the cleaned ITO glass and annealed at 423 K for 900 s in a dust-free atmosphere. The emitting layer (EML) was deposited by spin-coating the HY-PPV solution (6 mg/1 ml toluene) on top of the PEDOT:PSS layer at 6000 rpm and annealed at 65 ^{o}C for 25 min to remove the residual solvent. The electron-injection layer was cast on top of the EML by the spin-coating (1 mg/ml in ethanol) of the **3OTAZ**. Finally, the aluminum (90 nm) was deposited as the cathode by thermal evaporation at about 1 × 10^{-6} Torr. The current-luminance-voltage (I-L-V) characteristics of the devices were recorded using a combination of a Keithley power source (model 2400) and an Ocean Optics usb2000 fluorescence spectrophotometer. Current efficiency and luminous power efficiency were calculated from the I-L-V characteristics. The fabrication of the devices was done in ambient conditions, with the following performance tests conducted in a glove-box filled with nitrogen.

Results and discussion

Characterization of Electron-injection Material 3OTAZ

The electron-injection material **3OTAZ** was synthesized from 3,4,5-tris(4-fluorophenyl)-4*H*-1,2,4-triazole (**3**) and 2-(2-ethoxyethoxy)ethanol by the nucleophilic substitution reaction (Scheme 1). The chemical structure of **3OTAZ** had been well characterized by ^{1}H NMR spectra and elemental analysis (in Supporting Information),

whereas its optical properties were investigated by absorption spectroscopy (UV/Vis) and photoluminescence spectroscopy (PL). Glass transition temperatures (T_g) and thermal decomposition temperatures (T_d) (at 5 wt% loss) of **3OTAZ** were evaluated with differential scanning calorimetry (DSC) and thermal gravimetric analysis (TGA), respectively. Cyclic voltammetry (CV) was used to measure onset reduction and oxidation potentials of **3OTAZ** film, which in turn were used to estimate the LUMO and HOMO levels respectively.

Thermal Properties

Glass transition temperatures (T_g) and thermal decomposition temperatures (T_d) (at 5 wt% loss) of **3OTAZ** were evaluated with differential scanning calorimetry (DSC) and thermal gravimetric analysis (TGA) respectively, with the representative data summarized in Table 1. The melting point (T_m) of **3OTAZ** was observed at 67 °C (Figure S4 in SI), but no obvious glass transition temperature (T_g) and crystallization temperature (T_c) was detected between 30°C and 300 °C. This is due to three diethylene glycol ether groups of **3OTAZ** which effectively prevent close packing between the molecules. In addition, thermal decomposition temperature at 5% weight loss was quite high (376 ^{o}C) (Figure 1), indicating that **3OTAZ** is thermally stable to be applied in PLEDs.

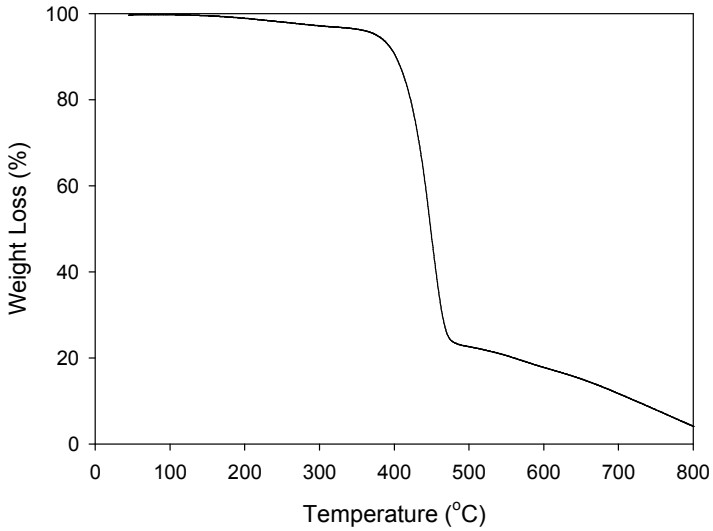

Figure 1. Thermogravimetric curves of **3OTAZ** at a heating rate of 10 °C/min under nitrogen atmosphere.

Table 1. Thermal, optical and electrochemical properties of **3OTAZ**.

Material	T_m[a] /T_d[b] (°C)	UV-vis λ_{max}/PL λ_{max} (nm)	$E_{onset(ox)}$ *vs.* FOC (V)[e]	$E_{onset(red)}$ *vs.* FOC (V)[e]	E_{HOMO}/E_{LUMO} (eV)[f]	E_g^{elg}/ E_g^{opth} (eV)
3OTAZ	67/376	272[c] (286, 347, 375)[d]/356[c] (358)[d]	1.06	-1.92	-5.86/-2.88	2.98/3.62

[a] Melting point determined by DSC measurement.

[b] The decomposition temperature at 5 wt% loss was measured by TGA at a heating rate of 10 °C/min under nitrogen.

[c] In ethanol (1×10^{-5}M).

[d] film state.

[e] E_{FOC} = 0.49 V vs. Ag/AgCl.

[f] E_{HOMO} = - ($E_{onset(ox),\ FOC}$ + 4.8) eV; E_{LUMO} = - ($E_{onset(red),\ FOC}$ + 4.8) eV.

[g] E_g^{el} = |LUMO-HOMO|: electrochemically estimated band-gap.

[h] $E_g^{opt} = 1240/\lambda_{onset(abs.\ spectrum)}$ (nm): optically estimated band-gap.

Optical Properties

Figure 2 illustrates the absorption and photoluminescence (PL) spectra of **3OTAZ** in solution (ethanol) and as film spin-coated from ethanol solution, with the characteristic optical data summarized in Table 1. The absorption maxima of **3OTAZ** are peaked at *ca.* 272 nm and 286 nm (with shoulders at 347 nm and 375 nm) in ethanol and as film, respectively. The major absorption of **3OTAZ** (*ca.* 272 nm and 286 nm) can be attributed to the π-π* transitions of 1,2,4-triazoly moieties, whereas the shorter-wavelength absorptions in the film state (*ca.* 347 nm and 375 nm) is probably originated from the n-π* transitions between diethylene glycol monoethyl ether moieties and 1,2,4-triazoly core.[30] The PL spectra of **3OTAZ** in solution and solid state locate at *ca.* 356 nm and *ca.* 358 nm, respectively. The absorption and PL maxima of **3OTAZ** in solid state (286 nm and 358 nm) are red-shifted slightly relative to solution state (272 nm and 356 nm), probably due to excimer formation via intra- or inter-chain interactions.[30a-e]

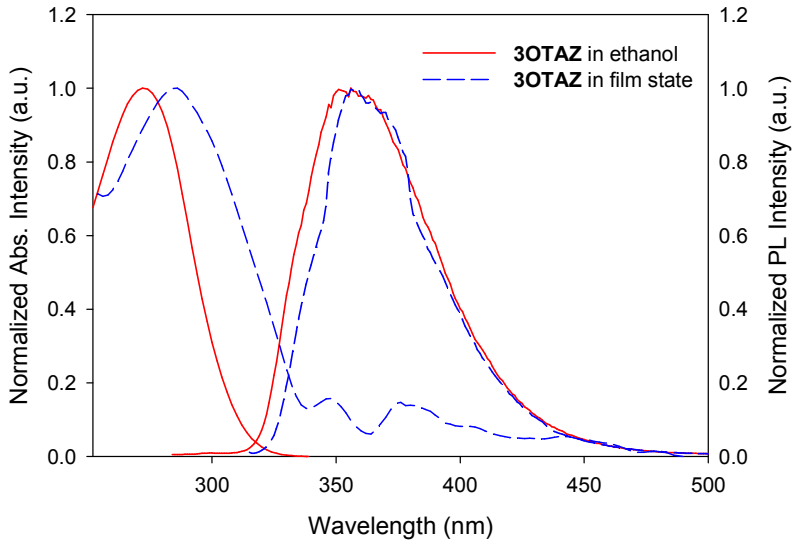

Figure 2. Absorption and photoluminescence spectra of **3OTAZ** in ethanol solution (λ_{ex} = 272 nm) and film state (λ_{ex} = 286 nm).

Electrochemical Properties

Cyclic voltammetry (CV) was employed to investigate the electrochemical properties of **3OTAZ**. The cyclic voltammograms of **3OTAZ** dissolved in 0.1M *n*-Bu_4NClO_4 are shown in Figure 3, with the representative electrochemical data summarized in Table 1. The HOMO and LUMO energy levels were estimated by the equations: E_{HOMO} (eV) = − ($E_{ox,FOC}$ + 4.8) and E_{LUMO} (eV) = − ($E_{red,FOC}$ + 4.8), where $E_{ox,FOC}$ and $E_{red,FOC}$ are the onset oxidation and onset reduction potentials, respectively, relative to the ferrocene/ferrocenium couple whose energy level is already known (-4.8 eV). The HOMO and LUMO energy levels of **3OTAZ** were estimated to be -5.86 eV and -2.88 eV respectively, as well as electrochemical band-gap (E_g^{el}) being 2.98 eV.

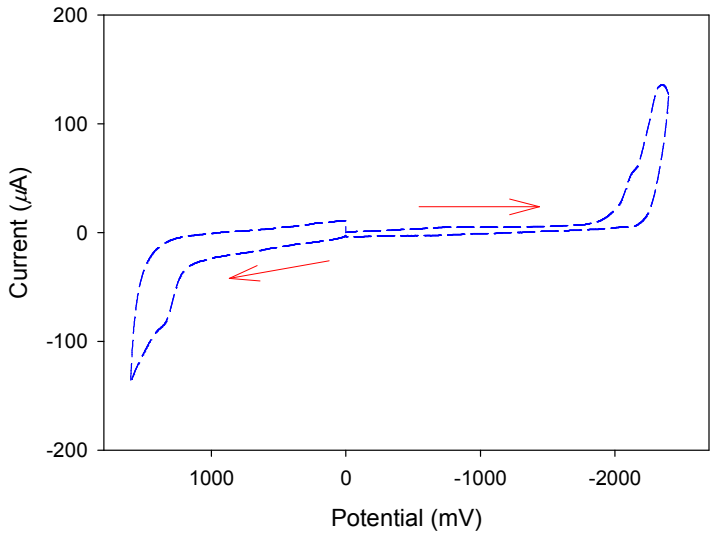

Figure 3. Cyclic voltammogram of **3OTAZ** dissolved in acetonitrile with 0.1M *n*-Bu_4NClO_4. Working electrode: glassy carbon, scan rate: 100 mV/s.

On the other hand, the optical band-gap ($E_g^{opt.}$) was estimated to 3.62 eV from the main onset absorption wavelength (343 nm) of **3OTAZ** in the film state (Figure 2). The energy band-gaps obtained by optical method and cyclic voltammetry were 2.98 eV and 3.62 eV, respectively. Electrochemically-estimated band-gap (E_g^{el}), calculated using $E_g^{el} = |LUMO - HOMO|$, is slightly different from optical band-gap (E_g^{opt}) obtained from onset absorption.

The electrochemical band-gap (E_g^{el}) is the energy difference between the LUMO and HOMO levels, which in turn are estimated from the onset oxidation and reduction potentials, respectively. However, oxidation and reduction may start from different parts of a molecule which is composed of electron-donating and electron-withdrawing groups. Therefore, the discrepancy between the band-gaps determined electrochemically (E_g^{el}) and optically (E_g^{opt}) is probably due to their different techniques to estimate the gaps. Due to **3OTAZ** is comprised of 1,2,4-triazoly core and three diethylene glycol monoethyl ether, oxidation may start from the electron-donating diethylene glycol monoethyl ether parts, and reduction may start from the 1,2,4-triazoly core of **3OTAZ**.

Electroluminescent Enhancement of PLEDs by inserting 3OTAZ

According to the energy band diagrams depicted in Figure 4, the energy barrier between aluminum (A1) and HY-PPV (2.5 eV) is larger than that between PEDOT:PSS and HY-PPV (0 eV). Moreover, holes are usually more readily transported than electrons in conjugated materials, leading to reduced recombination ratio of holes and electrons. Similar nonmatching energy barriers for electrons and holes are also apparent for the HY-PPV based device (Figure 4). However, the charge injection/transport imbalance in HY-PPV can be alleviated by inserting the electron injection and hole-blocking layer **3OTAZ** in which both LUMO and HOMO energy levels are lower than those of HY-PPV. The lowered LUMO and HOMO levels give rise to enhanced electron injection/transport and hole-blocking, respectively, resulting in more balanced charges recombination.

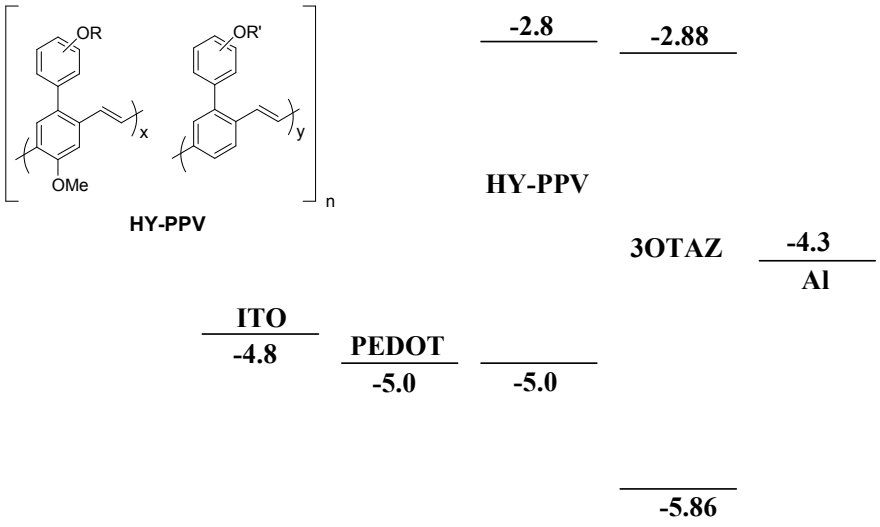

Figure 4. The energy band diagrams of **3OTAZ** and HY-PPV, with those of PEDOT:PSS, and electrodes.

Multi-layer polymer light-emitting diodes (PLEDs) with a configuration of ITO/PEDOT:PSS/EML (HY-PPV)/EIL/Al (90 nm) were fabricated to investigate their electroluminescent characteristics. In this work, we propose the use of a water/alcohol-soluble **3OTAZ** as electron injection layer (EIL) in a PLED with HY-PPV as the EML. The EIL was deposited on top of the EML by spin-coating of **3OTAZ** solution (1 mg **3OTAZ**/ml) using various spin speed (1000, 2000 and 3000 rpm). Current density–luminance–voltage (J–L–V) and luminous efficiency–power efficiency–current density (LE–PE–J) characteristics of the devices are shown in Figure 5 and Figure 6-7, with the corresponding optoelectronic data summarized in Table 2. The device performance is effectively enhanced by inserting the electron-injection layer (**3OTAZ**) between emitting layer (HY-PPV) and Al cathode.

Maximum luminance and current efficiency of devices were greatly increased from 230 cd/m^2 and 0.02 cd/A (0.006 lm/W) to 2970 cd/m^2 and 0.91 cd/A (0.34 lm/W), respectively, by inserting the electron-injection layer (EIL: **3OTAZ** with 3000 rpm spin speed) between emitting layer and Al cathode (Figure 5 and Figure 6-7). Although the performance

enhancement is inferior to that obtained with a conventional LiF/Al cathode, the **3OTAZ** effectively promote the device performance.[30l] The performance enhancement is probably attributed to the hole-blocking and improved electron injection effect of **3OTAZ** that raises charges recombination ratio. The HOMO level of **3OTAZ** (-5.86 eV) is much lower than that of emitting layer HY-PPV (-5.0 eV), resulting in blocking and accumulation of holes in the HY-PPV layer close to the interface. Moreover, the lower LUMO level of **3OTAZ** (-2.88 eV) than emitting layer HY-PPV (-2.8 eV) promotes electron injection (Figure 4). Therefore, holes will readily combine with electrons passing through the interface to increase the recombination ratio.

As shown in Table 2, the device with **3OTAZ** as EIL spin-coated at 3000 rpm reveals the best performance. Moreover, the turn-on voltages of the device decreases to 4.2 V which is much lower than 8.3 V obtained for that without **3OTAZ** as EIL. The electroluminescent enhancement is ascribed to effectively promoted electron injection/transport with **3OTAZ** as EIL that leads to higher charges recombination ratio. However, more homogeneous surface morphology of the EIL spin-coated at 3000 rpm (Figure S6 in SI: RMS roughness = 1.65 nm) also contributes to the performance improvement. In addition, the 1931 CIE coordinates (*x*, *y*) of the EL emission only shift slightly from (0.35, 0.60) to (0.41, 0.57) when the **3OTAZ** is inserted as EIL (Table 2), indicating that the emission of all devices is exclusively originated from HY-PPV.

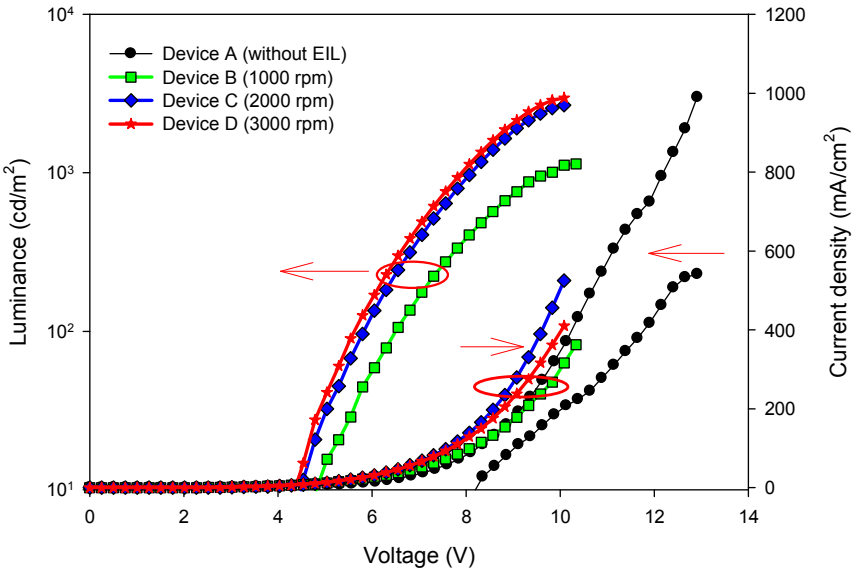

Figure 5. Luminance versus voltage and current density versus voltage characteristics of PLEDs. Device structure: ITO/PEDOT:PSS/HY-PPV/**3OTAZ**/Al.

Table 2. Optoelectronic Properties of the Light-emitting Diodes[a]

EIL	Thickness of EIL (nm)	V_{on} (V)[b]	L_{max} (cd/m^2)[c]	CE_{max} (cd/A)[d]	LPE_{max} (lm/W)[e]	CIE (x, y)[f]
None	—	8.2	230	0.02	0.006	(0.35, 0.60)
1000 rpm	87	4.8	1140	0.43	0.16	(0.40, 0.58)
2000 rpm	79	4.2	2670	0.71	0.27	(0.41, 0.57)
3000 rpm	60	4.3	2970	0.91	0.34	(0.41, 0.57)

[a] [ITO/PEDOT:PSS/HY-PPV (~80 nm)/EIL/Al (90nm)].

[b] Turn-on voltage at 10 cd/m^2.

[c] Maximum luminance.

[d] Maximum current efficiency.

[e] Maximum luminous power efficiency.

[f] The 1931 CIE coordinate at maximum luminance.

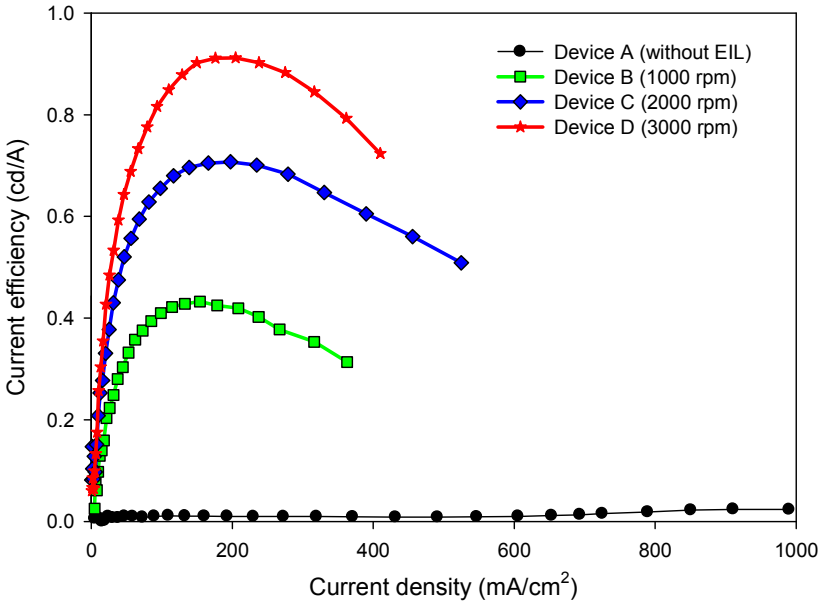

Figure 6. Current efficiency versus current density characteristics of PLEDs. Device structure: ITO/PEDOT:PSS/HY-PPV/**3OTAZ**/Al.

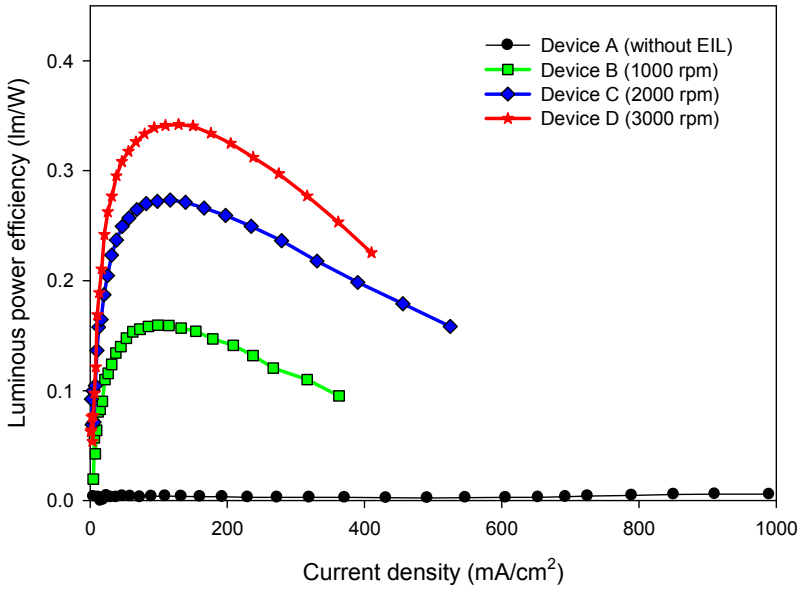

Figure 7. Luminous power efficiency versus current density characteristics of PLEDs. Device structure: ITO/PEDOT:PSS/HY-PPV/**3OTAZ**/Al.

To clarify the hole-blocking effect of EIL (**3OTAZ**), hole-only devices

[ITO/PEDOT:PSS/HY-PPV/EIL/Au (100 nm)] were fabricated to investigate their current density versus bias characteristics. As shown in Figure 8, the curve shifts horizontally to higher bias after the insertion of **3OTAZ** as EIL, indicating diminished current density under the same bias. The device using **3OTAZ** (spin speed: 1000, 2000 and 3000 rpm) as EILs reveal the similar current density, indicating that the hole-blocking effect is induced by inserting **3OTAZ**. However, the voltage-induced current densities are still lower than that of the device without EIL. Therefore, more balanced charges injection and transport was achieved by inserting EIL **3OTAZ** which adjust hole-blocking.

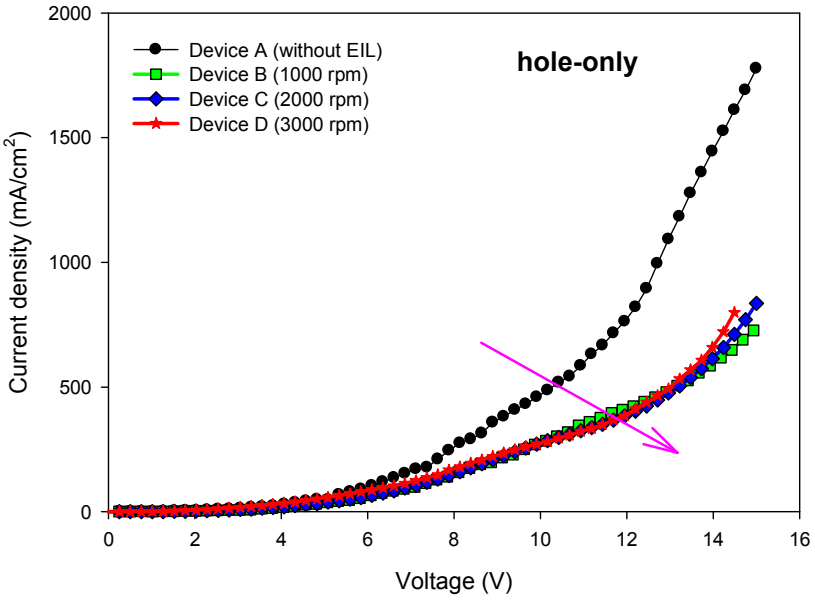

Figure 8. Current density versus voltage characteristics of hole-only PLEDs. Device structure: ITO/PEDOT:PSS/HY-PPV/EIL/Au.

To demonstrate the electron injection ability of the EIL (**3OTAZ**), electron-only devices [Glass/PEDOT:PSS/Ag (100 nm)/HY-PPV/EIL/A1 (90 nm)][33,34] were fabricated to

investigate their current density versus bias characteristics (Figure 9). The current density (under the same bias) is raised by the EILs, especially in the devices using the **3OTAZ (**spin speed: 3000 rpm**)** as EIL reveal the highest current density. This is attributed to enhancement in electron injection/transport by the **3OTAZ**. This suggests that the **3OTAZ (**spin speed: 3000 rpm**)** is the most effective EIL to promote electron injection/transport and more balance charges injection and transport.

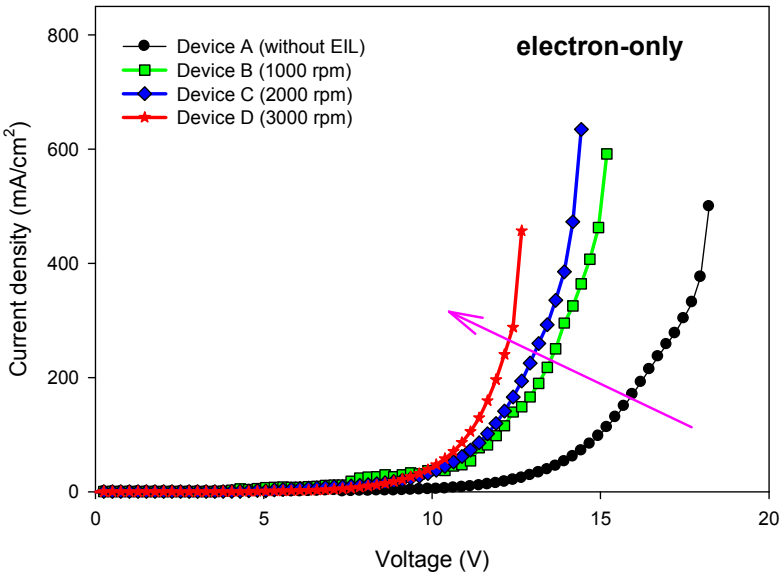

Figure 9. Current density versus voltage characteristics of electron-only PLEDs. Device structure: ITO/PEDOT:PSS/Ag/HY-PPV/EIL/Al.

Photovoltaic (PV) measurements were conducted to elucidate that addition of **3OTAZ** plays crucial role in promoting electron injection in the PLEDs. When the anode is kept identical (ITO/PEDOT:PSS), the open-circuit voltage (V_{oc}) is primarily determined by effective work-function of the cathode, which reflects the electron-injection ability of the EIL materials.[11,35] The V_{oc} was 1.32 V for the device based on HY-PPV without EIL, respectively, which was increased to 1.45 V when the **3OTAZ** was inserted as the EIL

(Figure 10). Higher V_{oc} means that the built-in potential (the difference in work function between anode and cathode) across its anode/EML/cathode junction has been increased. Therefore, a drop in the work function of EIL/Al cathode (or generation of interfacial dipoles at the EIL/metal junction) has been realized by inserting the EIL. Lower work function of cathode usually facilitates electron injection. Accordingly, the significant performance enhancement in devices using the **3OTAZ** as EIL should be mainly due to enhanced electron-injection ability. Current results indicate that aromatic 1,2,4-triazole-based **3OTAZ** with diethylene glycol monoethyl ether groups is not only an effective hole-blocking material but also a promising stable cathode modifier in promoting electron injection and device performance.

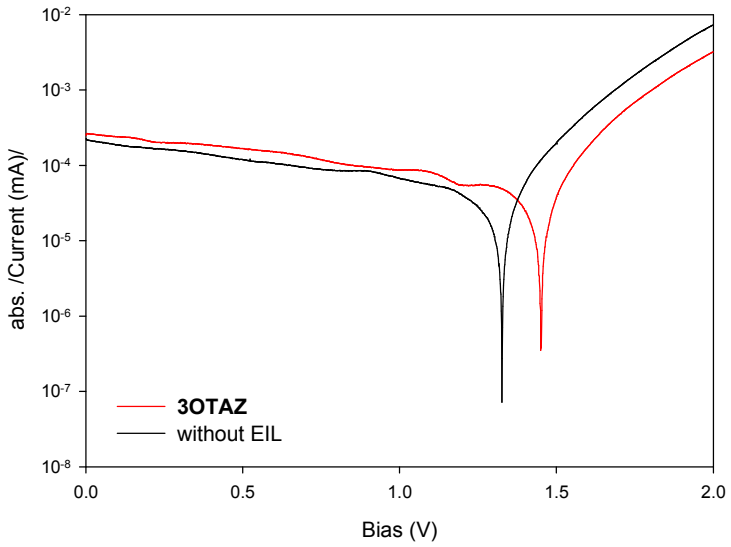

Figure 10. Photovoltaic measurements of PLEDs using **3OTAZ** as electron injection layer under illumination from a solar simulator (Newport, Oriel class A, 91160A) at 100% sun (AM1.5, 100 mW/cm^2). Device structure: ITO/PEDOT:PSS/HY-PPV/EIL/Al.

Conclusion

We have presented a novel aromatic 1,2,4-triazole-based **3OTAZ** with diethylene glycol monoethyl ether groups as electron-injection layer (EIL) and hole-blocking layer for

fabrication of multilayer PLEDs by spin-coating process. The **3OTAZ** was a highly efficient EIL to more balance charge injection/transport. The devices based on HY-PPV as emission layer with **3OTAZ** (spin speed: 3000 rpm) as EIL (ITO/PEDOT:PSS/HY-PPV/EIL/Al) revealed the best device performance. Maximum luminance and current efficiency of devices were 2970 cd/m^2 and 0.91 cd/A (0.34 lm/W), respectively, which were superior to those without electron injection layer [230 cd/m^2 and 0.02 cd/A (0.006 lm/W)]. In addition, the turn-on voltage of the device was decreased to 4.2 V which is much lower than 8.3 V obtained for those without **3OTAZ** as EIL. The electron- and hole-only devices and their open circuit voltages (V_{oc}) had been investigated to clarify their charges injection/transport abilities and the influence of **3OTAZ** in electroluminescence. The performance enhancement has been attributed to promoted electron injection/transport and hole-blocking effect by the inserted **3OTAZ**. Current results demonstrate that **3OTAZ** is an effective electron injection/transport material applicable to optoelectronic devices.

Supporting Information

Synthesis and characterization of monomers, the COSY and NOESY NMR spectra of **3OTAZ**, and surface AFM images of **3OTAZ** thin film.

Acknowledgment

This research received funding from the Headquarters of University Advancement at the National Cheng Kung University, which is sponsored by the Ministry of Education, Taiwan, ROC.

References and Notes

(1) J. H. Burroughes, D. D. C. Bradley, A. R. Brown, R. N. Marks, K. Mackey, R. H. Friend, P. L. Burn, A. B. Holmes, *Nature* **1990**, 347, 539.

(2) J. R. Sheats, H. Antoniadis, M. Hueschen, W. Leonard, J. Miller, R. Moon, D. B. Roitman, A. Stocking, *Science* **1996**, 273, 884.

(3) R. H. Friend, R. W. Gymer, A. B. Holmes, J. H. Burroughes, D. D. C. Bradley, D. A. D.

Santos, J. L. Bredas, M. Loglund, W. R. Salaneck, *Nature* **1999**, 397, 121.

(4) *Organic Light-Emitting Devices: synthesis, properties and applications*; K. Mullen, U. Scherf, Eds.; Wiley-VCH: Weinheim, **2006**.

(5) Y. Z. Lee, X. Chen, S. A. Chen, P. K. Wei, W. S. Fann, *J. Am. Chem. Soc.* **2001**, 123, 2296.

(6) F. Garten, A. Hilberer, F. Cacialli, E. Esselink, Y. V. Dam, B. Schlatmann, R. H. Friend, T. M. Klapwijk, G. Hadziioannou, *Adv. Mater.* **1997**, 9, 127.

(7) J. S. Kim, R. H. Friend, F. Cacialli, *Appl. Phys. Lett.* **1999**, 74, 3084.

(8) Q. Huang, G. Evmenenko, P. Dutta, P. Lee, N. R. Armstrong, T. J. Marks, *J. Am. Chem. Soc.* **2005**, 127, 10227.

(9) S. Kato, *J. Am. Chem. Soc.* **2005**, 127, 11538.

(10) D. Braun, A. J. Heeger, *Appl. Phys. Lett.* **1991**, 58, 1982.

(11) H. Wu, F. Huang, Y. Mo, W. Yang, D. Wang, J. Peng, Y. Cao, *Adv. Mater.* **2004**, 16, 1826.

(12) T.-W. Lee, H.-C. Lee, O. O. Park, *Appl. Phys. Lett.* **2002**, 81, 214.

(13) (a) X. Y. Deng, W. M. Lau, K. Y. Wong, K. H. Low, H. F. Chow, Y. Cao, *Appl. Phys. Lett.* **2004**, 84, 3522. (b) T. F. Guo, F. S. Yang, Z. J. Tsai, T. C. Wen, S. N. Hsieh, Y. S. Fu, *Appl. Phys. Lett.* **2005**, 87, 13504.

(14) G. Hughes, M. R. Bryce, *J. Mater. Chem.,* **2005**, 15, 94.

(15) S. H. Jin, M. Y. Kim, J. Y. Kim, K. Lee, Y. S. Gal, *J. Am. Chem. Soc.* **2004**, 126, 2474.

(16) F. Huang, H. B. Wu, D. L. Wang, W. Yang, Y. Cao, *Chem. Mater.* **2004**, 16, 708.

(17) F. Huang, Y. H. Niu, Y. Zhang, J. W. Ka, M. S. Liu, A. K. Y. Jen, *Adv. Mater.* **2007**, 19, 2010.

(18) F. Huang, Y. Zhang, M. S. Liu, A. K. Y. Jen, *Adv. Funct. Mater.* **2009**, 19, 2457.

(19) S. H. Oh, D. Vak, S. I. Na, T. W. Lee, D. Y. Kim, *Adv. Mater.* **2008**, 20, 1624.

(20) R. Yang, H. Wu, Y. Cao, G. C. Bazan, *J. Am. Chem. Soc.* **2006**, 128, 14422.

(21) C. V. Hoven, A. Garcia, G. C. Bazan, T. Q. Nguyen, *Adv. Mater.* **2008**, 20, 3793.

(22) X. Xu, B. Han, J. Chen, J. Peng, H. Wu, Y. Cao, *Macromolecules* **2011**, 44, 4204.

(23) F. Huang, P. I. Shih, C. F. Shu, Y. Chi, Alex K.-Y. Jen, *Adv. Mater.* **2009**, 21, 361

(24) C. J. Pedersen, *J. Am. Chem. Soc.* **1967**, 89, 2495.

(25) C. J. Pedersen, *Angew. Chem., Int. Ed. Engl.* **1988**, 27, 1021.

(26) H. H. Lu, Y. S. Ma, N. J. Yang, G. H. Lin, Y. C. Wu, S. A. Chen, *J. Am. Chem. Soc.* **2011**, 133, 9634.

(27) (a) Y. H. Niu, H. Ma, Q. Xu, A. K-Y. Jen, *Appl. Phys. Lett.* **2005**, 86, 083 504. (b) Y. H. Niu, A. K.-Y. Jen, C. F. Shu, *J. Phys. Chem. B* **2006**, 110, 6010.

(28) (a) M. Strukelj, F. Papadimitrakopoulos, T. M. Miller and L. J. Rothberg, *Science* **1995**, 267, 1969. (b) A. W. Grice, A. Tajbakhsh, P. L. Burn and D. D. C. Bradley, *Adv. Mater.* **1997**, 9, 1174.

(29) (a) C. Adachi, M. A. Baldo, S. R. Forrest and M. E. Thompson, *Appl. Phys. Lett.* **2000**, **77**, 904. (b) S.-H. Chen and Y. Chen, *Macromolecules* **2005**, 38, 53. (c) T. Yasuda, T. Imase, Y. Nakamura and T. Yamamoto, *Macromolecules* **2005**, 38, 4687.

(30) (a) C.-S. Wu and Y. Chen, *Macromolecules*, **2009**, 42, 3729. (b) C.-S. Wu and Y. Chen, *J. Mater. Chem.,* **2010**, 20, 7700. (c) C.-S. Wu and Y. Chen, *J. Polym. Sci. Part A Polym. Chem.*, **2010**, 48, 5727. (d) C.-S. Wu, S.-L. Lee and Y. Chen, *J. Polym. Sci. Part A Polym. Chem.*, **2011**, 49, 3099. (e) C.-S. Wu and Y. Chen, *J. Polym. Sci. Part A Polym. Chem.*, **2011**, 49, 3928. (f) C.-S. Wu, Y.-J. Yang, S.-W. Fang and Y. Chen, *J. Polym. Sci. Part A Polym. Chem.*, 2012, **50**, 3875 (g) C.-S. Wu, Y.-T. Lee and Y. Chen, Y. *Polym. Chem.*, **2012**, 3, 2776. (h) C.-S. Wu, C.-T. Liu and Y. Chen, Y. *Polym. Chem.*, **2012**, 3, 3308. (i) C.-S. Wu, J.-W. Wu and Y. Chen, *J. Mater. Chem.,* **2012**, 22, 23877. (j) C.-S. Wu, C.-P. Chen and Y. Chen, *J. Polym. Sci. Part A Polym. Chem.*, **2013**, 51, 3975. (k) C.-S. Wu, S.-W. Fang and Y. Chen, *Phys. Chem. Chem. Phys.*, **2013**, 15,15121. (l) C.-S. Wu, H.-A. Lu, Y.-J. Lin and Y. Chen, *J. Mater. Chem. C,* **2013**, 1, 6850. (m) C.-S. Wu,

Y.-J. Lin and Y. Chen *Org. Biomol. Chem.,* **2014**, 12, 1419. (n) C.-S. Wu, H.-A. Lu, C.-P. Chen, T.-F. Guo and Y. Chen *Org. Biomol. Chem.,* **2014**, 12, 1430.

(31) T. H. Lee, J. C. A. Huang, T. F. Guo, T. C. Wen,Y. S. Huang, C. C. Tsou, C. T. Chung, Y. C. Lin, Y. J. Hsu, *Adv. Funct. Mater.* **2008**, 16, 3036.

(32) L. Scholer, K. Seibel, K. Panczyk, M. Bohm, *Microelectron. Eng.* **2009**, 86, 1502.

(33) K. Manabe, W. Hu, M. Matsumura, H. Naito, *J. Appl. Phys.* **2003**, 94, 2024.

(34) R. Steyrleuthner, S. Bange, D. Neher, *J. Appl. Phys.* **2009**, 105, 064509.

(35) L. S. Yu, S. A. Chen, *Adv. Mater.* **2004**, 16, 744.